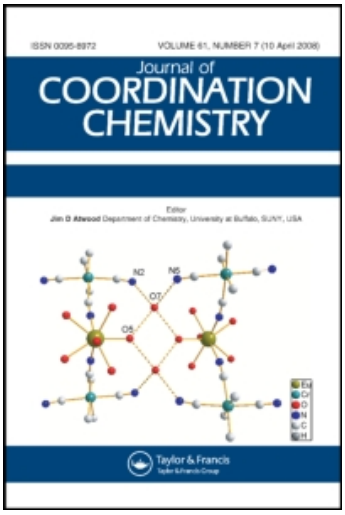

Journal of Coordination Chemistry
Publication details, including instructions for authors and subscription information:
http://www.informaworld.com/smpp/title~content=t713455674

Theoretical and experimental study of the electronic structure and spectra of Ni(II) tetraazadinaphtho[14]annulene complexes

Ángel Ríos-Escudero[a]; Guillermina L. Estiú[b]; Juan Costamagna[a]; Gloria I. Cárdenas-Jirón[a]
[a] Departamento de Química de los Materiales and Departamento de Ciencias Químicas, Facultad de Química y Biología, Universidad de Santiago de Chile, Santiago, Chile [b] Departamento de Química Inorgánica, Analítica y Química Física, Facultad de Ciencias Exactas y Naturales, Universidad de Buenos Aires, Ciudad Universitaria, Buenos Aires C1428EHA, Argentina

Online publication date: 12 May 2010

To cite this Article Ríos-Escudero, Ángel , Estiú, Guillermina L. , Costamagna, Juan and Cárdenas-Jirón, Gloria I.(2003) 'Theoretical and experimental study of the electronic structure and spectra of Ni(II) tetraazadinaphtho[14]annulene complexes', Journal of Coordination Chemistry, 56: 14, 1257 — 1267
To link to this Article: DOI: 10.1080/00958970310001624276
URL: http://dx.doi.org/10.1080/00958970310001624276

J. Coord. Chem. Vol. 56, No. 14, 20 September 2003, pp. 1257–1267

THEORETICAL AND EXPERIMENTAL STUDY OF THE ELECTRONIC STRUCTURE AND SPECTRA OF Ni(II) TETRAAZADINAPHTHO[14]ANNULENE COMPLEXES

ÁNGEL RÍOS-ESCUDERO[a], GUILLERMINA L. ESTIÚ[b,*], JUAN COSTAMAGNA[a,†] and GLORIA I. CÁRDENAS-JIRÓN[a,†]

[a]*Departamento de Química de los Materiales and Departamento de Ciencias Químicas, Facultad de Química y Biología, Universidad de Santiago de Chile, Casilla 40, Correo 33, Santiago, Chile;* [b]*Departamento de Química Inorgánica, Analítica y Química Física, Facultad de Ciencias Exactas y Naturales, Universidad de Buenos Aires, Pabellón 2, Ciudad Universitaria, Buenos Aires C1428EHA, Argentina and Departamento de Química, Cequinor, Facultad de Ciencias Exactas, Universidad Nacional de La Plata, 47 esq. 115, La Plata (B1900AVV), Argentina*

(Received 10 December 2002; In final form 24 August 2003)

A theoretical and experimental study of the acid–base equilibrium of Ni^{II}tetraazadinaphtho[14]annulene complex (NiN_4CH_3) with their corresponding four protonated derived species ($NiN_4CH_3H_2^{2+}$) is presented. Geometry optimizations have been carried out at a PM3(tm) semiempirical level, whereas UV-visible transitions have been calculated using the ZINDO/S-CI method parameterized for spectroscopy, and further compared with the experimental spectra. We found very good agreement between the predicted spectrum for the NiN_4CH_3 complex and the experimental one. Among the protonated $NiN_4CH_3H_2^{2+}$ species, $NiN_4CH_3H_2$*trans*,*trans*$^{2+}$ has the best agreement with experiment. The results have allowed us to identify the conformational characteristics of the protonated structures, for which a *trans*,*trans* position of the hydrogen atoms relative to the naphthalene moiety is favored.

Keywords: Ni(II) complexes; Azamacrocycles; ZINDO/S-CI; Electronic spectra

INTRODUCTION

Macrocyclic complexes have attracted research interest as valuable bioinorganic mimics of the catalytic centers for the active sites occurring in hemoproteins and metalloenzymes [1–7]. They are also important for their analytical, biological and catalytic applications, largely related to supramolecular chemistry and materials science [8–12].

*Present address: Department of Chemistry, 152 Davey Laboratory, The Pennsylvania State University, University Park, PA 16802, USA.

†Corresponding authors. E-mail: gcardena@lauca.usach.cl; jcostama@lauca.usach.cl

ISSN 0095-8972 print: ISSN 1029-0389 online © 2003 Taylor & Francis Ltd
DOI: 10.1080/0095897031000162427 6

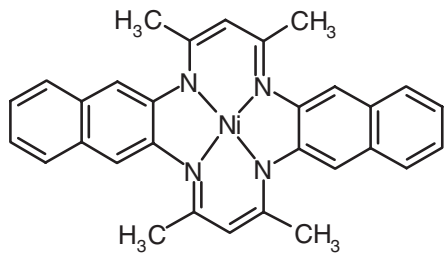

FIGURE 1 Molecular structure of the Ni^{II}tetraazadinaphtho[14]annulene (NiN_4CH_3) complex.

Since the synthesis of tetraazadibenzo[14]annulene macrocycles by Jäger in 1962 [13], several complexes have been synthesized with different transition metals and also different substituents in the ligand [14–19]. These macrocyclic compounds were recognized as synthetic model systems capable of activating small molecules (O_2, CO, CO_2) as in porphyrins and corrins [20, 21]. Among the synthetic macrocycles derived from tetraazadibenzo[14]annulene, those containing the tetraazadinaphtho[14]annulene system [22, 23] (see Fig. 1) are particularly interesting because of their extended π conjugated system which plays an important role in the electro- and photoactivation of small substrates. The catalytic properties of these systems are associated with electron transfer processes that involve π electrons delocalized in the macrocycle, d electrons of the metal center and charge transfer transitions between them. Because of this, research on these systems usually requires a thorough analysis of their associated electronic spectra.

The electronic spectra of metal complexes allows not only characterization of their structure but also interpretation of changes in their reactivity in processes that involve electronic excitations in electron transfer processes [24, 25]. Quantum chemical calculations have become a valuable tool for studying and predicting structural and spectroscopic properties of macrocyclic ligands and their metal complexes [26–30]. We present in this article an experimental and theoretical study of the acid–base equilibrium established between Ni^{II}tetraazadinaphtho[14]annulene (NiN_4CH_3) and the protonated Ni^{II}tetraazadinaphtho[14]annuleneH_2^{2+} ($NiN_4CH_3H_2^{2+}$) complexes:

$$NiN_4CH_3 + 2H^+ \equiv NiN_4CH_3H_2^{2+}.$$

The study is based on the characterization of the ground state geometry of the metal complexes, i.e., the NiN_4CH_3 species and the four structural isomers associated with the $NiN_4CH_3H_2^{2+}$ protonated species, followed by calculation of their corresponding UV-visible spectra by means of configuration interaction (CI) techniques. Comparative analysis of the experimental and theoretical results has allowed a thorough understanding of the processes that occur in the Ni^{II}tetraazadinaphtho[14]annulene acid–base equilibrium.

COMPUTATIONAL DETAILS

The geometries of the NiN_4CH_3 structure and the four $NiN_4CH_3H_2^{2+}$ protonated structural isomers (see Fig. 2) have been fully optimized without restrictions at a

semiempirical PM3(tm) (transition metal) level (TITAN package [31]). Protonation has been considered to occur on either the methylenic carbons (see Fig. 2B) as well as on the nitrogen atoms. In the latter, cis and trans orientations relative to the naphthalene moiety have been considered, defining $NiN_4CH_3H_2$*cis*,*trans*$^{2+}$, $NiN_4CH_3H_2$*cis*,*cis*$^{2+}$ and $NiN_4CH_3H_2$*trans*,*trans*$^{2+}$ isomers (see Figs. 2C, 2D and 2E, respectively). The structures were optimized as either closed shell (RHF, Restricted Hartree–Fock) singlet state electronic configurations, or open shell (UHF, Unrestricted Hartree–Fock) triplet state configurations when necessary. Optimizations of triplet states were performed whenever the geometries converged to tetrahedrally distorted structures, as justified below (see Structure). The electronic spectra were calculated using the INDO model [27, 32–34] parameterized for spectroscopy, at the configuration interaction singles (CIS) level of theory (ZINDO/S-CI) [27,35–37]. The calculations generated a number of singly excited configurations that varied from

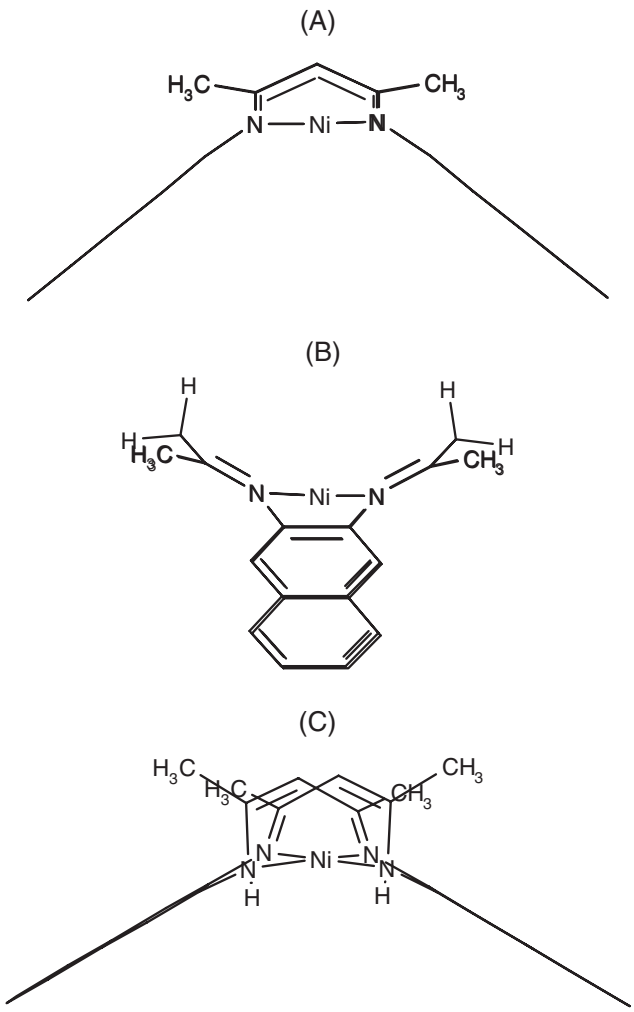

FIGURE 2 Optimized molecular structure at the PM3(tm) level of theory: (A) NiN_4CH_3; (B) $NiN_4CH_3H_2inC^{2+}$; (C) $NiN_4CH_3H_2$*cis*,*cis*$^{2+}$; (D) $NiN_4CH_3H_2$*cis*,*trans*$^{2+}$ and (E) $NiN_4CH_3H_2$*trans*,*trans*$^{2+}$.

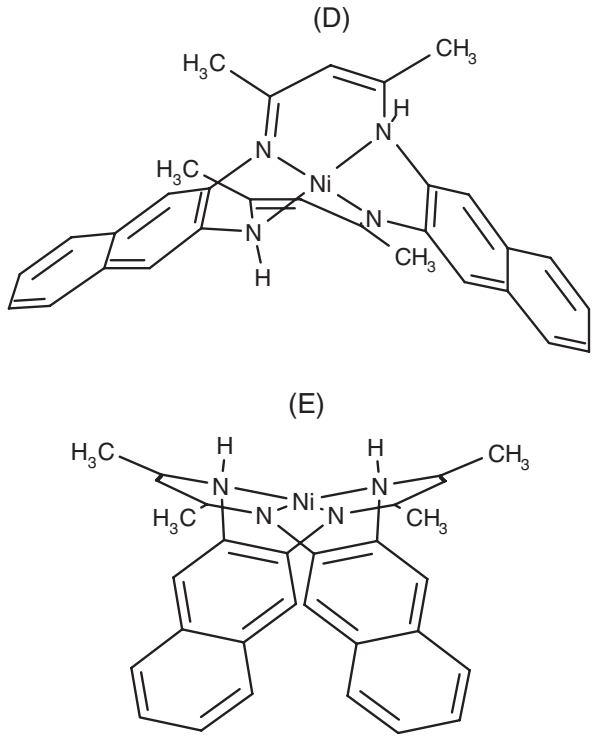

FIGURE 2 Continued.

244 to 1045, depending on the species studied. The size of CIS resulted from inclusion of transitions involving the higher energy 27 to 32 occupied molecular orbitals and the lower energy 9 to 13 virtual molecular orbitals, depending again on the system under consideration. The occupied and virtual molecular orbitals involved in single excitations were chosen, for each of the structures, as those containing π and d contributions in the linear combination of atomic orbitals that define them.

RESULTS AND DISCUSSION

Structure

The chemical equilibrium shown above involves NiN_4CH_3 and the $NiN_4CH_3H_2^{2+}$ protonated species. The results of the theoretical calculations obtained for the molecules in the singlet and triplet states of the N–Ni–N and N(H)–Ni–N(H) angles are shown in Table I. The N(H)–Ni–N(H) angle is defined for molecules protonated on the nitrogen atoms. In the NiN_4CH_3 complex (see Fig. 2A) the NiN_4 center is nearly planar with two N–Ni–N angles of 176°. The same occurs in the $NiN_4CH_3H_2inC^{2+}$ complex (see Fig. 2B), where the two hydrogen atoms bonded to the methylenic carbons and the NiN_4 moiety define an almost planar substructure with the N–Ni–N angle being 178°. The other $NiN_4CH_3H_2^{2+}$ structural isomers, when calculated as singlet states, converge to geometries where the NiN_4 center is almost planar, but showing a slight

TABLE I Theoretical N–Ni–N and N(H)–Ni–N(H) angles calculated at PM3(tm) semiempirical level corresponding to the NiN_4 center

Species	*Singlet state*		*Triplet state*	
	N–Ni–N	*N(H)–Ni–N(H)*	*N–Ni–N*	*N(H)–Ni–N(H)*
NiN_4CH_3	176	–	–	–
$NiN_4CH_3H_2inC^{2+}$	178	–	–	–
$NiN_4CH_3H_2$*cis*,*cis*$^{2+}$	173	168	173	166
$NiN_4CH_3H_2$*cis*,*trans*$^{2+}$	176	173	178	175
$NiN_4CH_3H_2$*trans*,*trans*$^{2+}$	162	160	166	169

distortion that we named *pseudo*-tetrahedral distortion, i.e., N–Ni–N = 173° and N(H)–Ni–N(H) = 168° for $NiN_4CH_3H_2$*cis*,*cis*$^{2+}$ (see Fig. 2C) N–Ni–N = 176° and N(H)–Ni–N(H) = 173° for $NiN_4CH_3H_2$*cis*,*trans*$^{2+}$ (see Fig. 2D), and N–Ni–N = 162° and N(H)–Ni–N(H) = 160° for $NiN_4CH_3H_2$*trans*,*trans*$^{2+}$ (see Fig. 2E). These angles represent a distortion relative to the plane defined by the NiN_4 center, that ranges between 7 and 20°. Similar distortions result from the calculations for triplet state structures which are summarized in Table I.

Since square planar Ni(II) complexes are generally diamagnetic, the ground states of the NiN_4CH_3 and $NiN_4CH_3H_2inC^{2+}$ species have only been studied as singlet states. Tetrahedral Ni(II) complexes, on the other hand, are known to be paramagnetic. Therefore, for the $NiN_4CH_3H_2$*trans*,*trans*$^{2+}$, $NiN_4CH_3H_2$*cis*,*cis*$^{2+}$ and $NiN_4CH_3H_2$*cis*,*trans*$^{2+}$ species, singlet and triplet states were compared in order to account for the small tetrahedral distortion associated with these isomers.

Electronic Spectra

UV-visible spectra in methanol (1×10^{-3} M in NiN_4CH_3) with aliquots of 0.1 M perchloric acid were recorded using a Varian Cary 1 E spectrophotometer. The equilibrium established between the NiN_4CH_3 and the $NiN_4CH_3H_2^{2+}$ complexes was followed, for the direct reaction, by the pH change of the methanolic solution, for which values between 2.3 and 7.8 were determined. For each pH value, the UV-visible spectrum was recorded and compared with the initial spectrum corresponding to the NiN_4CH_3 species. The presence of $NiN_4CH_3H_2^{2+}$ becomes evident as a dramatic change in the UV-visible spectrum (pH = 5.9), that occurs with a change in the color of the solution. A graph of the titration curve is inserted in Fig. 3. The inverse reaction, i.e., the reaction from $NiN_4CH_3H_2^{2+}$ to NiN_4CH_3, has also been carried out in order to verify that a chemical equilibrium was established. The UV-visible spectra of the NiN_4CH_3 and the $NiN_4CH_3H_2^{2+}$ complexes, shown in Fig. 3, exhibit several bands in the region between 350 and 600 nm. The position and intensity of the absorption bands are shown in Table II. Differences in the electronic spectra of both species exist. For NiN_4CH_3 there are only three bands: a high-intensity band at 400 nm, a band of lower intensity at 450 nm and a broad feature in the region of 550–600 nm. On the other hand, for $NiN_4CH_3H_2^{2+}$ six bands are observed in the same region, as reported in Table II. The differences in the electronic spectra, together with a knowledge of the structural characteristics of protonated and non-protonated species, has prompted our theoretical study of the UV-visible spectra, directed towards a full understanding of the events involved in the associated mechanism.

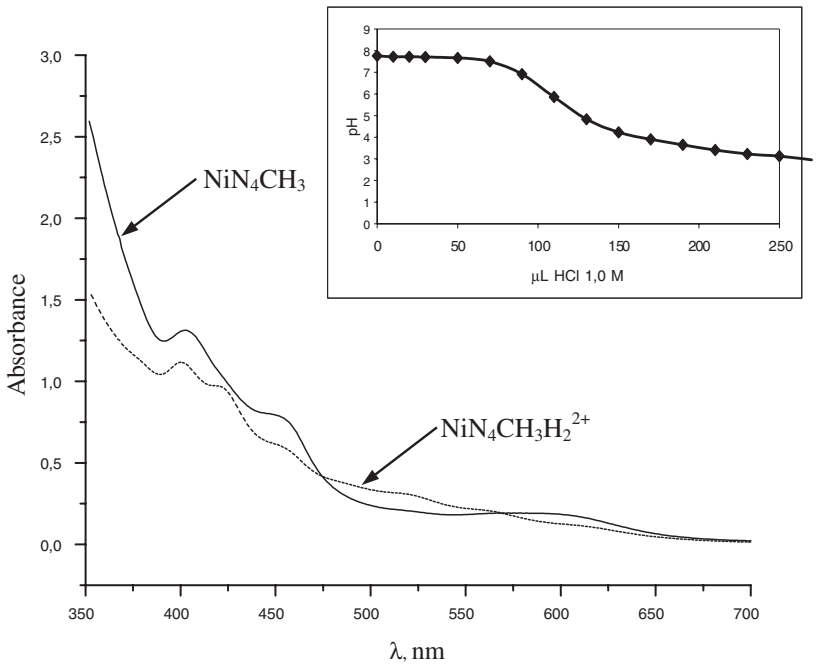

FIGURE 3 Experimental UV-visible spectra of the NiN_4CH_3 and $NiN_4CH_3H_2^{2+}$ species; (insert) the titration curve.

TABLE II Experimental bands of NiN_4CH_3 and $NiN_4CH_3H_2^{2+}$

Band	*NiN_4CH_3*		*NiN_4CH_3 H_2^{2+}*	
	λ (nm)	ε ($M^{-1}cm^{-1}$)	λ (nm)	ε ($M^{-1}cm^{-1}$)
1	400	1400	395	1200
2	450	800	430	1000
3	550–600	200	450	700
4			475	400
5			515	350
6			565	300

The calculated data, on which the assignments were established, are also reported for all of the molecules in Tables III–VII. In this section we analyze the nature of the observed electronic transitions for the NiN_4CH_3 and the $NiN_4CH_3H_2^{2+}$ complexes using the ZINDO/S-CI methodology [34]. The calculated electronic spectra, together with the theoretical assignments of the corresponding bands, are reported in Table III for the NiN_4CH_3 species. The experimental spectrum is dominated by a strong transition at 400 nm, which we associate with the contribution of two theoretical bands, one of high intensity at 412 nm, and another of lower intensity at 410 nm. The former results from an intra-ligand ($\pi \rightarrow \pi^*$) transition from a π orbital delocalized over the methylenic carbon and the nitrogen atoms, to an anti-bonding π, this time delocalized on the methylenic and azomethynic carbon atoms. The latter excitation is assigned to a metal-to-ligand charge transfer (MLCT) transition, from a $3d_{yz}$ orbital of the metal

TABLE III Calculated electronic spectra of NiN_4CH_3 at the ZINDO/S-CI level of theory

λ (nm)	f[a]	*Transition*	*Assignment*
410	0.0096	S → S	79 → 89 (44%), d → $\pi_{C(C=N)}$
			86 → 93 (38%), $\pi_{naph} \rightarrow \pi_{naph}$
			84 → 94 (37%), $\pi_{met} \rightarrow \pi_{naph}$
412	0.0268	S → S	87 → 99 (65%), $\pi_{met\text{-}N} \rightarrow \pi_{met\text{-}C(C=N)}$
			85 → 95 (46%), π_{naph} → d
			88 → 98 (39%), $\pi_{met\text{-}N} \rightarrow \pi_{naph\text{-}C(C=N)}$
447	0.0108	S → S	85 → 95 (69%), π_{naph} → d
			88 → 98 (37%), $\pi_{met\text{-}N} \rightarrow \pi_{naph\text{-}C(C=N)}$
566	0.0017	S → S	84 → 89 (41%), d,$\pi_{met} \rightarrow \pi_{C(C=N)}$
			87 → 94 (39%), $\pi_{met\text{-}N} \rightarrow \pi_{naph}$
			88 → 97 (32%), $\pi_{met\text{-}N} \rightarrow \pi_{naph}$
598	0.0022	S → S	86 → 90 (57%), $\pi_{met} \rightarrow \pi_{C(C=N)}$
			82 → 89 (51%), d → $\pi_{C(C=N)}$
			88 → 93 (44%), $\pi_{met\text{-}N} \rightarrow \pi_{naph}$
599	0.0049	S → S	86 → 90 (60%), $\pi_{met} \rightarrow \pi_{C(C=N)}$
			82 → 89 (56%), d → $\pi_{C(C=N)}$

[a]Oscillator strength.

TABLE IV Calculated electronic spectra of $NiN_4CH_3H_2inC^{2+}$ at the ZINDO/S-CI level of theory

λ (nm)	f[a]	*Transition*	*Assignment*
357	0.2084	S → S	87 → 91 (54%), $\pi_{naph} \rightarrow \pi_{C(C=N)}$
			88 → 89 (72%), $\pi_{naph} \rightarrow \pi_{C(C=N)}$

[a]Oscillator strength.

TABLE V Calculated electronic spectra of $NiN_4CH_3H_2$*cis*,*cis*$^{2+}$ at the ZINDO/S-CI level of theory

λ (nm)	f[a]	*Transition*	*Assignment*
362	0.0412	T → T	89 → 90 (50%), $\pi_{C(C=N)} \rightarrow \pi_{C(C=N)}$
			87 → 90 (36%), $\pi_{naph} \rightarrow \pi_{C(C=N)}$
368	0.0080	T → T	70 → 91 (58%), d → d
373	0.1090	T → T	86 → 91 (37%), $\pi_{naph} \rightarrow \pi_{met\text{-}N}$
			79 → 88 (36%), d → $\pi_{met\text{-}N}$
376	0.1853	T → T	87 → 90 (73%), $\pi_{naph} \rightarrow \pi_{C(C=N)}$
387	0.0601	T → T	87 → 90 (53%), $\pi_{naph} \rightarrow \pi_{C(C=N)}$
			89 → 90 (50%), $\pi_{C(C=N)} \rightarrow \pi_{C(C=N)}$
426	0.0051	T → T	77 → 91 (37%), d → d
			74 → 91 (33%), d → d
440	0.0782	T → T	86 → 93 (50%), $\pi_{naph} \rightarrow \pi_{naph}$
445	0.0064	T → T	85 → 88 (43%), $\pi_{naph} \rightarrow \pi_{met\text{-}N}$
			70 → 91 (33%), d → d
451	0.0186	T → T	85 → 88 (63%), $\pi_{naph} \rightarrow \pi_{met\text{-}N}$
458	0.0061	S → S	84 → 91 (50%), π_{met}, d → d
			72 → 91 (49%), d → d
462	0.0055	T → T	80 → 91 (43%), d → d
470	0.1307	T → T	88 → 92 (54%), $\pi_{C(C=N)} \rightarrow \pi_{C(C=N)}$, π_{met}
			84 → 88 (36%), $\pi_{naph} \rightarrow \pi_{met\text{-}N}$
481	0.0015	T → T	87 → 94 (40%), $\pi_{naph} \rightarrow \pi_{naph}$
502	0.0043	S → S	83 → 91 (52%), d → d
			81 → 91 (42%), d → d
			80 → 91 (41%), d → d
520	0.0021	T → T	87 → 88 (91%), $\pi_{naph} \rightarrow \pi_{met\text{-}N}$

[a]Oscillator strength.

TABLE VI Calculated electronic spectra of $NiN_4CH_3H_2$*cis*,*trans*$^{2+}$ at the ZINDO/S-CI level of theory

λ (nm)	f[a]	*Transition*	*Assignment*
391	0.2567	S → S	88 → 89 (71%), $\pi_{met} \rightarrow \pi_{C(C=N)}$
			88 → 90 (43%), $\pi_{met} \rightarrow \pi_{C(C=N)}$
392	0.0398	T → T	85 → 90 (89%), $\pi_{naph} \rightarrow \pi_{C(C=N)}$
393	0.0475	S → S	71 → 91 (50%), d → d
			70 → 91 (33%), d, $\pi_N \rightarrow$ d
426	0.0025	S → S	77 → 91 (69%), d → d
			72 → 91 (47%), d → d
442	0.0182	T → T	87 → 88 (74%), $\pi_{naph} \rightarrow$ d
			85 → 88 (38%), $\pi_{naph} \rightarrow$ d
449	0.0040	S → S	78 → 91 (68%), d → d
472	0.0276	T → T	87 → 90 (50%), $\pi_{naph} \rightarrow \pi_{C(C=N)}$
522	0.2622	T → T	87 → 90 (87%), $\pi_{naph} \rightarrow \pi_{C(C=N)}$
539	0.0025	T → T	86 → 93 (43%), $\pi_{naph} \rightarrow \pi_{C(C=N)}$, π_{met}
562	0.0110	T → T	87 → 97 (39%), $\pi_{naph} \rightarrow \pi_{naph}$

[a]Oscillator strength.

TABLE VII Calculated electronic spectra of $NiN_4CH_3H_2$*trans*,*trans*$^{2+}$ at the ZINDO/S-CI level of theory

λ (nm)	f[a]	*Transition*	*Assignment*
394	0.0659	T → T	87 → 91 (47%), $\pi_{naph} \rightarrow \pi_{C(C=N)}$
			87 → 91 (42%), $\pi_{naph} \rightarrow \pi_{C(C=N)}$
			86 → 91 (39%), $\pi_{naph} \rightarrow \pi_{C(C=N)}$
395	0.1329	T → T	87 → 91 (45%), $\pi_{naph} \rightarrow \pi_{C(C=N)}$
			87 → 91 (43%), $\pi_{naph} \rightarrow \pi_{C(C=N)}$
			86 → 91 (40%), $\pi_{naph} \rightarrow \pi_{C(C=N)}$
430	0.0174	T → T	86 → 91 (39%), $\pi_{naph} \rightarrow$ d
439	0.0369	T → T	87 → 90 (50%), $\pi_{naph} \rightarrow \pi_{C(C=N)}$
			87 → 90 (40%), $\pi_{naph} \rightarrow \pi_{C(C=N)}$
			70 → 89 (36%), d → d
440	0.0023	S → S	71 → 91 (58%), d → d
			68 → 91 (48%), d → d
444	0.0230	T → T	70 → 89 (47%), d → d
			72 → 89 (43%), d → d
457	0.0070	T → T	86 → 96 (36%), $\pi_{naph} \rightarrow \pi_{naph}$
			86 → 94 (33%), $\pi_{naph} \rightarrow \pi_{naph}$
474	0.0506	T → T	87 → 90 (67%), $\pi_{naph} \rightarrow \pi_{C(C=N)}$
			87 → 90 (46%), $\pi_{naph} \rightarrow \pi_{C(C=N)}$
508	0.0442	T → T	87 → 88 (59%), $\pi_{naph} \rightarrow$ d
556	0.0020	S → S	72 → 91 (50%), d → d
			86 → 91 (38%), $\pi_{naph} \rightarrow$ d
580	0.0038	S → S	80 → 91 (70%), d → d
			81 → 91 (37%), d, $\pi_{naph} \rightarrow$ d

[a]Oscillator strength.

center to one π of the ligand, mainly delocalized on the $2p_y$ orbitals of the azomethynic carbon atoms. The band in the UV-visible spectrum at 450 nm is calculated at 447 nm and assigned to a ligand-to-metal charge transfer (LMCT) transition from a π of the aromatic system of naphthalene to the $3d_{xz}$ orbital on the Ni atom. In relation to the experimental band occurring between 550 and 600 nm, we found three bands (566 nm, 598 nm and 599 nm) associated with a mixture of $\pi \rightarrow \pi^*$ and MLCT transitions that can account for this feature.

For the protonated species, the singlet state for $NiN_4CH_3H_2$ in C^{2+} (Table IV), and both singlet and triplet configurations for $NiN_4CH_3H_2$*cis*,*cis*$^{2+}$ (Table V), $NiN_4CH_3H_2$*cis*,*trans*$^{2+}$ (Table VI) and $NiN_4CH_3H_2$*trans*,*trans*$^{2+}$ (Table VII) have been analyzed according to the results of the optimization procedures (see Structure). For each of these geometries the electronic spectrum has been calculated.

From comparative analysis of the electronic spectra of the protonated species it has become evident that the one belonging to the $NiN_4CH_3H_2$*trans*,*trans*$^{2+}$ species shows the best agreement with experiment. This conclusion is based not only on the coincidence in the position of the experimental and calculated bands on the energy scale but also on the similarity of the relative intensities, which are estimated in the theoretical spectra through calculations of the oscillator strengths from the dipole length operator [34]. The spectra predicted for the $NiN_4CH_3H_2$*cis*,*cis*$^{2+}$ and $NiN_4CH_3H_2$*cis*,*trans*$^{2+}$ species only show good agreement with experiment for some of the bands. In the case of $NiN_4CH_3H_2$*cis*,*cis*$^{2+}$ species, the calculations successfully predict the four experimental bands of higher energy, developing at 395, 430, 450 and 475 nm. However, the oscillator strengths calculated for them do not correlate accurately with the trend observed for the extinction coefficients. For the $NiN_4CH_3H_2$*cis*,*trans*$^{2+}$ species, we found good correlation between the predicted wavelengths and the ones appearing in the experimental spectrum, but complete disagreement between the trend obtained for the oscillator strengths and the experimental intensities. On the other hand, the spectrum predicted for the $NiN_4CH_3H_2$inC^{2+} species shows no agreement with the experimental one, regardless of the energy region considered. These results led us to conclude that the $NiN_4CH_3H_2$*trans*,*trans*$^{2+}$ species is responsible for the experimental spectroscopic features and hence is the "predominant" or even the "unique" protonated species involved in the chemical equilibrium.

The calculated electronic spectrum of the $NiN_4CH_3H_2$*trans*,*trans*$^{2+}$ species shows several bands that correlate with the experimental bands, whose energy, intensity and theoretical assignment are reported in Table VII. The well-defined experimental band at 395 nm results from the contribution of two bands, calculated at 394 nm and at 395 nm, corresponding to triplet–triplet excitations, and assigned to $\pi \rightarrow \pi^*$ transitions from a delocalized orbital of naphthalene to an unoccupied orbital centered on the azomethyne carbon. The band of lower intensity that develops at 430 nm in the UV-visible spectrum is interpreted as belonging to a mixture of three bands: two corresponding to triplet–triplet excitations, at 430 and 439 nm, and one band corresponding to a singlet–singlet excitation at 440 nm. All show strong mixtures of LMCT, d-d and $\pi \rightarrow \pi^*$ excitations. The experimental band at 450 nm is mainly assigned to d-d excitations on the basis of the calculations, which relate it to triplet–triplet transitions, at 444 and 457 nm. The bands developing at 475 and 515 nm in the experimental spectrum are associated with calculated transitions at 474 and 508 nm, respectively. These bands belong to pure triplet–triplet $\pi \rightarrow \pi^*$ and triplet–triplet LMCT transitions, respectively. The former band results from a transition starting in π orbitals of the conjugated system of naphthalene and ending in the $2p_y$ orbitals of the azomethylenic carbon atoms. The latter band corresponds to a transition from the same π orbitals of naphthalene to the $3d_{x^2-y^2}$ orbital of the metal center. A mixture of two bands, at 556 and 580 nm, accounts for the last experimental band appearing at 565 nm. They belong to singlet–singlet transitions involving d-d excitations. The band at 556 nm corresponds to a transition between the $3d_{yz}$ and the $3d_{xz}$ orbitals of the metal

center, whereas the one at 580 nm corresponds to a transition from the $3d_{x^2-y^2}$ metal orbital to the $3d_{xz}$ one.

We conclude from the previous analysis that the electronic transitions in the UV-visible spectrum of the protonated species originate in triplet–triplet transitions occurring in the $NiN_4CH_3H_2$*trans*,*trans*$^{2+}$ molecular system. This conclusion supports the results from the geometry optimization of this species, which indicate a *pseudo*-tetrahedral distortion, characteristic of Ni(II) complexes of high multiplicity.

CONCLUSION

The electronic spectra of the species that define the acid–base equilibrium (NiN_4CH_3 and $NiN_4CH_3H_2^{2+}$ complexes) have been studied by means of theoretical and experimental procedures. Only one isomer is associated with the non-protonated species, and experiment and theory show perfect agreement in this case. On the other hand, four different protonated isomers can contribute to the equilibrium. Nevertheless, from a comparison of the spectra calculated for each of them with the experimental one, we concluded that the $NiN_4CH_3H_2$*trans*,*trans*$^{2+}$ isomer could be the one involved in the equilibrium. The analysis of the UV-visible spectrum for this isomer shows major triplet–triplet contributions, supporting the results of the geometry optimization procedures, which converge to a species with a *pseudo*-tetrahedral distortion, characteristic of high-spin Ni complexes.

Acknowledgements

JC and GICJ would like to acknowledge financial support from Project FONDECYT Lineas Complementarias N° 8010006/2002. GICJ also thanks Vicerrectoría de Investigación y Desarrollo (USACH) for the position of Research Associate. ARE thanks CONICYT, DIGEGRA (USACH) and RELAQ for a graduate fellowship. GLE is a member of the scientific staff of the Argentine Research Council (Conicet), Argentina.

References

[1] J. Costamagna, J. Vargas, R. Latorre, A. Alvarado and G. Mena, *Coord. Chem. Rev.* **119**, 67 (1992).
[2] E.J. Barán, Química Bioinorgánica (McGraw Hill, Madrid, 1994), pp. 177–181.
[3] I. Zilbermann, G. Golub, H. Cohen and D. Meyerstein, *Inorg. Chim. Acta.* **227**, 1 (1994).
[4] R. Cammack, *Nature* **390**, 443 (1997).
[5] U. Ermler, W. Grabarse, S. Shima, M. Goubeaud and R. Thauer, *Science* **278**, 1457 (1997).
[6] J. Trommel, K. Warncke and L. Marzilli, *J. Am. Chem. Soc.* **123**, 3358 (2001).
[7] H.M. Marques and K.L. Brown, *Coord. Chem. Rev.* **225**, 123 (2002).
[8] J. Trommel, K. Warncke and L. Marzilli, *J. Am. Chem. Soc.* **123**, 3358 (2001).
[9] N. Herron and D.H. Busch, *J. Am. Chem. Soc.* **103**, 1236 (1981).
[10] I. Bhugun, D. Lexa and J.-M. Savéant, *J. Am. Chem. Soc.* **118**, 1769 (1996).
[11] J. Grodkowski, T. Dhanasekaran, P. Neta, P. Hambright, B. Brunschwig, K. Shinozaki and E. Fujita, *J. Phys. Chem.* **104**, 11332 (2000).
[12] V. Amendola, L. Fabbrizzi, M. Licchelli, C. Mangano, P. Pallavicini, L. Parodi and A. Poggi, *Coord. Chem. Rev.* **190–192**, 649 (1999).
[13] E.G. Jäger, *Z. Anorg. Allg. Chem.* **364**, 177 (1969).
[14] F.A. Cotton and J. Czuchajowska, *Polyhedron* **9**, 2553 (1990).

[15] L. Giannini, E. Solari, S. de Angelis, T.R. Ward, C. Floriani, A. Chiesi-Villa and C. Rizzoli, *J. Am. Chem. Soc*. **117**, 5801 (1995).
[16] D.G. Black, R.F. Jordan and R.D. Rogers, *Inorg. Chem*. **36**, 103 (1997).
[17] G.I. Nikonov, A.J. Blake and P. Mountford, *Inorg. Chem*. **36**, 1107 (1997).
[18] P. Mountford, *Chem. Soc. Rev*. **27**, 105 (1998).
[19] J. Eilmes, M. Ptaszek and K. Wozniak, *Polyhedron* **21**, 7 (2002).
[20] V.L. Goedken, S.M. Reng, J.A. Molin-Norris and Y. Park, *J. Am. Chem. Soc*. **93**, 85 (1976).
[21] H. Brand and J. Arnold, *Coord. Chem. Rev*. **140**, 137 (1995).
[22] J. Costamagna, G. Ferraudi, M. Villagran and E. Wolcan, *J. Chem. Soc*., *Dalton Trans*. 2631 (2000).
[23] C.R. Olave, E.A.F. Carrasco, M. Campos-Vallette, M.S. Saavedra, G.F. Diaz, R.E. Clavijo, W. Figueroa, J.V. García-Ramos, S. Sánchez-Cortez, C. Domingo, J. Costamagna and A. Ríos-Escudero, *Vib. Spectrosc*. **28**, 287 (2002).
[24] M.G. Cory and M.C. Zerner, *Chem. Rev*. **91**, 813 (1991).
[25] H.E. Toma, R.M. Serrasqueiro, R.C. Rocha, G.J.F. Demets, H. Winnischofer, K. Araki, P.E.A. Ribeiro and C.L. Donnici, *J. Photochem. Photobiol. A*: *Chem*. **135**, 185 (2000).
[26] G.L. Estiú, A.H. Jubert, J. Molina, J. Costamagna, J. Canales and J. Vargas, *Inorg. Chem*. **34**, 1212 (1995).
[27] G.L. Estiú and M.C. Zerner, *J. Am. Chem. Soc*. **121**, 1893 (1999).
[28] J. Canales, J. Ramirez, G. Estiú and J. Costamagna, *Polyhedron* **19**, 2373 (2000).
[29] Md. K. Nazeeruddin, S.M. Zakeeruddin, R. Humphry-Baker, S.I. Gorelsky, A.B.P. Lever and M. Gratzel, *Coord. Chem. Rev*. **208**, 213 (2000).
[30] S.I. Gorelsky and A.B.P. Lever, *J. Organometallic Chem*. **635**, 187 (2001).
[31] TITAN 1.0.7, Wavefunction, Inc. and Schrodinger Inc., 18401 Von Karman Avenue, Suite 370, Irvine, CA 92612 USA.
[32] J.A. Pople, D.P. Santry and G.A. Segal, *J. Chem. Phys*. **43**, 129 (1965).
[33] J.A. Pople, D.L. Beveridge and P.A. Dobosh, *J. Chem. Phys*. **47**, 47 (1967).
[34] M.C. Zerner, ZINDO, Quantum Theory Project (University of Florida, Gainesville, FL, 1999).
[35] J. Ridley and M.C. Zerner, *Theor. Chim. Acta* **32**, 111 (1973).
[36] J. Ridley and M.C. Zerner, *Theor. Chim. Acta* **42**, 223 (1976).
[37] M.C. Zerner, G. Loew, R. Kirchner and U. Mueller-Westerhoff, *J. Am. Chem. Soc*. **102**, 589 (1980).